Simulations of antihydrogen formation

F. Robicheaux*
Department of Physics, Auburn University, Alabama 36849-5311, USA
(Received 31 October 2003; published 20 August 2004)

The results of simulations of antihydrogen formation in a Penning trap are reported. The antihydrogen atoms are formed by three-body capture. We find that the arrested nature of the three-body capture in the trap greatly reduces the expected binding energy of the antihydrogen. Typically, the formed antihydrogen has larger velocity along the magnetic field than across the field and a binding energy below k_BT.

DOI: 10.1103/PhysRevA.70.022510 PACS number(s): 36.10.−k, 32.60.+i, 34.80.Lx

I. INTRODUCTION

The formation of cold antihydrogen has been reported by the ATHENA [1] and ATRAP groups [2,3]. In both experiments, cold antiprotons, $\bar{p}$'s traverse a cold positron e^+ plasma; a $\bar{p}$ can capture one of the positrons during its brief time in the plasma. Presumably [4–6], the antihydrogen $\bar{H}$ is formed through three-body capture since this mechanism has the largest rate for the parameters of the experiments. In three-body capture, e^+'s scatter in the field of a $\bar{p}$ so that an e^+ loses enough energy to become bound to the $\bar{p}$. This paper reports the results of simulations incorporating several important processes that control the interaction of $\bar{p}$'s with a magnetized e^+ plasma. The simulations give insight into the properties of the $\bar{H}$ atoms that have been formed and insight into the mechanisms that control the $\bar{H}$ formation.

Both experimental configurations are based on the idea of nested Penning traps for the $\bar{p}$'s and e^+'s [4]. The traps consist of a long cylinder constructed from electrodes which can be held at different voltages; a strong magnetic field along the cylinder prevents the charged antiparticles from reaching the wall and annihilating. A schematic drawing of the $\bar{p}$ potential energy in the magnetic field direction is given in Fig. 1 of Ref. [1] and Fig. 2 of Ref. [2]. The voltages on the electrodes are chosen to give a double-well potential with the positrons trapped at the peak of the potential energy for a $\bar{p}$ (see Fig. 1).

The $\bar{p}$'s have a cyclotron period of roughly 10 ns and the period of oscillation along the **B** field is roughly 10 μs when the $\bar{p}$'s have sufficient energy to reach the e^+ plasma. The most important processes occur when a $\bar{p}$ crosses the top of the double-well potential where the e^+ plasma is trapped [7]. A $\bar{p}$ traveling through a magnetized e^+ plasma can lose energy through the excitation of plasma oscillations and through close collisions with individual e^+'s; this can heat the plasma [8]. While a $\bar{p}$ travels through the plasma, e^+'s can collide in the field of the $\bar{p}$ and one can be captured: a $\bar{H}$ is formed in a Rydberg state [4]. If the e^+ is bound deeply enough, the $\bar{H}$ will be able to survive the electric fields in the trap and either hit a wall and annihilate or travel to a detection region. If it is not deeply bound, the e^+ will be stripped from the atom; the $\bar{p}$ will change energy due to the potential difference between where the e^+ was captured and where it was stripped.

The short time that a $\bar{p}$ spends in the e^+ plasma strongly modifies the mechanism of three-body recombination; the modification is strong enough that it could be called by a different name: three-body capture. In the usual treatment (see Ref. [9] for $B=0$ and Refs. [5,6] for $B\neq 0$), it is assumed that the recombination is a steady-state process: e^+'s are continually interacting with a $\bar{p}$. The recombination rate is then the rate that e^+'s reach a certain binding energy. The three-body recombination rate is proportional to the square of the positron density times $T^{-9/2}$. But three-body recombination *is not a one-step process* (see Fig. 2). Typically, an e^+ will get captured to a state with a binding energy less than k_BT. Most often, the e^+ will be re-ionized due to collisions with other e^+'s. Sometimes, after many collisions, the e^+ will be scattered to a state with enough binding energy so that it is not re-ionized. *This takes time* [5,10]; most $\bar{H}$ atoms formed in the reported experiments are not in the e^+ plasma long enough for this process to complete. When the $\bar{p}$ leaves the e^+ plasma, the capture process is stopped—i.e., arrested. The simulations of *arrested* three-body capture presented in this paper give $\bar{H}$ atoms with binding energies much less than might otherwise be expected.

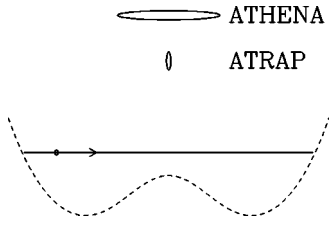

FIG. 1. Schematic drawing of the double-well potential for $\bar{p}$. The ellipses give the rough shape of the e^+ cloud in the two experiments. In the ATHENA experiments, the e^+ cloud has radius (across the magnetic field) of roughly 2–2.5 mm and a thickness (along the magnetic field) of roughly 32 mm. In the ATRAP experiments, the e^+ cloud has a radius of roughly 3 mm and a thickness of roughly 0.4–0.9 mm. The thickness has a strong effect on the three-body capture because the $\bar{p}$ can have a large speed through the plasma which means the $\bar{p}$ can only interact with the e^+ plasma for a short time. At 1 km/s, a $\bar{p}$ crosses the e^+ plasma in roughly 30 μs for the ATHENA configuration and roughly 0.5–1.0 μs in the ATRAP configuration.

*Electronic address: robicfj@auburn.edu

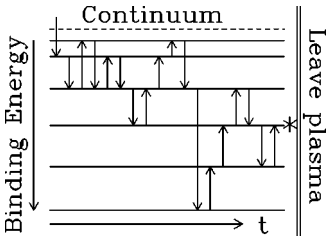

FIG. 2. Schematic drawing of the capture of an e^+. The e^+ is captured from the continuum at the left during a collision between two e^+'s in the field of a $\bar{p}$; the other e^+ carries away the lost energy. Usually, the $\bar{H}$ is initially bound by less than k_BT. Subsequent collisions with e^+'s in the plasma cause transitions to other states. When the $\bar{H}$ leaves the plasma, the transitions cease and the $\bar{H}$ has the energy marked by the asterisk. In steady state, $\bar{H}$ atoms bound by less than k_BT are usually ionized in subsequent collisions. If the $\bar{H}$ only spends a short time in the plasma, the binding energy will be much less than for steady-state recombination.

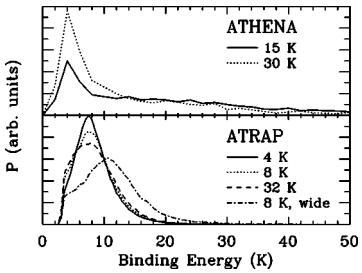

FIG. 3. The probability P for a $\bar{H}$ atom to have binding energy. All ATHENA simulations are for an e^+ density of 2.5×10^8 cm^{-3} and an extent of 32 mm along the magnetic field. All ATRAP simulations are for an e^+ density of 4×10^7 cm^{-3}; three simulations are for an extent of 0.4 mm along the magnetic field and one for an extent of 1.6 mm. To survive a 25 V/cm field, an atom needs a binding energy greater than ~40 K.

II. THREE-BODY CAPTURE

To simulate the arrested three-body capture, the classical equations of motion were numerically solved for e^+'s randomly (in time and space) fired at the $\bar{p}$; the phase space distribution of e^+'s matches that experienced by the $\bar{p}$ in the plasma. This procedure is described in Sec. II B of Ref. [6], but the e^+'s are only fired during a finite time interval matching the time the $\bar{p}$ spends in the plasma. The e^+'s move through a cube with an edge length of $x_{max}=10e^2/(4\pi\varepsilon_0 k_b T)$ with the $\bar{p}$ near the center of the cube. The number of e^+'s in the simulation varies since the number increases by 1 each time a new e^+ is fired into the cube and decreases by 1 each time an e^+ leaves the cube. The equations of motion for the e^+'s allow for full motion along the magnetic field but use the guiding center approximation (i.e., $\vec{E}\times\vec{B}$ drift) for motion across the magnetic field [Eqs. (1) of Ref. [6]]. By using this approximation we do not have to solve for the cyclotron motion of the e^+'s. The equations of motion for the $\bar{p}$ are not approximated.

When the $\bar{p}$ enters the e^+ plasma, the time that it spends in the plasma is computed from the $\bar{p}$ energy and its distance from the center of the trap. When the $\bar{p}$ leaves the plasma, no more e^+'s are fired. We continue propagating Newton's equations for a time given by $10x_{max}/\sqrt{k_BT/m}$ which is roughly $10\times$ the time needed for the average e^+ to cross the interaction volume. If an e^+ remains near the $\bar{p}$, then it has usually been captured and its binding energy is computed. Finally, we ramp an electric field along the magnetic field to numerically obtain the maximum field the $\bar{H}$ can survive. The ramp rate of the electric field is typically faster than that due to the motion through the trap but is slow enough so that the computed maximum field is accurate; this is accomplished by performing several runs with the ramp rate decreased by a factor of 2 after each run.

Figure 3 shows the simulated distribution of binding energies of $\bar{H}$ atoms formed in the two experiments. The arrested nature of the three-body capture dominates the distribution of binding energies: the binding energies are much less than the $8k_BT$ needed to stabilize atoms in a plasma [6]. There are several interesting features apparent in this graph. Three different temperatures give roughly the same distribution in the ATRAP experiment due to the short time available for the e^+-$\bar{H}$ collisions: a $\bar{p}$ traveling at 1 km/s can cross the plasma in less than 1 μs. The distribution shifts to deeper binding if the plasma is made thicker due to the increased chance of e^+-$\bar{H}$ collisions. The distribution extends to deeper binding for the ATHENA geometry due to the larger thickness and higher density of their plasma. Figure 3 shows that estimates from three-body recombination should be used with caution. For example, estimates give a factor of ~3 reduction in the recombination in a 30 K plasma that is 80 times thicker and 6.25 times denser than a 4 K plasma. However, comparing the data in Fig. 3 shows that the capture in the 30 K plasma is enhanced and the binding energy is larger. The only geometry that gave significant number of atoms bound by $8k_BT$ was the ATHENA geometry at 15 K; for this case, only 12% of the $\bar{p}$'s form $\bar{H}$ atoms bound by more than 120 K ($8k_BT$) while 20% of the $\bar{p}$'s form $\bar{H}$ atoms with binding energy between 40 K and 120 K; the remaining 68% of the $\bar{p}$'s form $\bar{H}$ atoms with binding energy less than 40 K which is not deep enough to survive the electric fields in the trap and thus these atoms will not reach the wall and annihilate.

The simulations give estimates for the number of $\bar{H}$ atoms that could be detected in each experiment. In both experiments, the $\bar{H}$ needs to survive roughly 25 V/cm field to be detected; this roughly corresponds to a binding energy of 40 K. In the ATHENA geometry, $\bar{H}$ atoms are detected when they reach the wall of the trap and annihilate. In the ATRAP geometry, the $\bar{H}$ atoms are detected in a region such that the $\bar{H}$ velocity along the magnetic field must be $8\times$ larger than velocity across the field. For the ATHENA geometry at 15 K, the simulation gave that 33% of the $\bar{p}$'s form $\bar{H}$ atoms that could reach the walls of the trap. Reference [11] reported $17\%\pm2\%$; the 17% is partly due to details of the trap and is not due to fundamental physics.

For the ATRAP geometry, the simulation gave smaller fractions of atoms that could survive a 25 V/cm field:

roughly 1/1000 at 4 K, 1/1400 at 8 K, and 1/1500 at 32 K. We performed simulations at different temperatures because the simulations (described below) indicate that the $\bar{p}$'s heat the e^+ plasma. From Fig. 4 of Ref. [2], the fraction of $\bar{p}$'s detected as $\bar{H}$ atoms is roughly 1/5000 for 5×10^5 e^+'s. To make a direct comparison to experiment, it is necessary to account for the travel of the $\bar{H}$ atoms to the detection region. Accounting for this, the simulation gives 1/16 000 at 4 K, 1/14 000 at 8 K, and 1/21 000 at 32 K.

The simulated $\bar{H}$ fraction is roughly a factor of 2 larger than measured for the ATHENA geometry and a factor of 3–4 smaller than the measurement for the ATRAP geometry. We feel this is good agreement since the fractions differed by roughly a factor of 1000 between the two experiments. Limitations of the simulations and uncertainties in the experimental plasma parameters are discussed below.

The steady-state three-body recombination rate is proportional to $T^{-9/2}$. Thus, it may be surprising that doubling the temperature for the ATHENA geometry decreased the $\bar{H}$ fraction by a factor of 2.6 instead of a factor of 23: at 30 K, 13% of the $\bar{p}$'s convert to detectable $\bar{H}$ atoms compared to 33% at 15 K. The reason for the difference is that this is not a steady-state experiment. A $\bar{p}$ continues to pass through the e^+ plasma until it captures an e^+. The only question is whether the binding energy will be sufficient to allow the $\bar{H}$ to reach the walls. So the temperature effect is more due to the branching ratio of capture energy than due to the speed with which the reaction occurs. Measurements also show a temperature dependence not as strong as $T^{-9/2}$ [12].

The binding energy might be expected to be proportional to T since the temperature is the only obvious energy scale for three-body capture. The binding energy for the ATRAP geometry shows little temperature dependence and the binding energy for the ATHENA geometry is *larger* for the 15 K plasma than for the 30 K plasma. Again this is due to the short time allowed for three-body capture. For the ATHENA geometry, this effect is probably due to the more rapid capture in the colder plasma; this gives a longer time for e^+-$\bar{H}$ scattering to drive the $\bar{H}$ atoms to more deeply bound states. Also, Coulomb cross sections decrease with increasing energy which means the e^+-$\bar{H}$ collisions are less effective in the 30 K plasma. This explanation is reminiscent of that given in Ref. [13] to explain the surprising distribution of Rydberg atom binding energies formed in ultracold plasmas [14]. For the ATRAP geometry, the distribution more nearly reflects the direct capture in a single step $e^+ + e^+ + \bar{p} \rightarrow e^+ + \bar{H}$ [15].

To test for the dependence on the thickness of the plasma, we calculated the capture at 8 K for the ATRAP geometry but the extent of the plasma along the field was taken to be 4× larger. For this simulation, 1/220 $\bar{p}$'s form atoms that can survive a 25 V/cm field and 1/2300 atoms would reach the detection region: roughly 6× larger than for the thinner plasma. Also, the energy distribution shifts to much deeper binding, Fig. 3.

The dependence of the binding energy on the thickness of the e^+ plasma was investigated for the arrangement in Ref. [3]. A thickness of 3.1 mm was used to match recent measurements [16] where $\bar{H}$ atoms were observed to survive 360 V/cm fields. For the 8 K plasma, the distribution of binding energy is clearly much deeper although it is still peaked at weak binding energy; a small fraction (less than 5%) of simulated $\bar{H}$ atoms survive a 100 V/cm field and a very small fraction (less than 1%) survive a 300 V/cm field. The simulation does not give as many $\bar{H}$ atoms as deeply bound as the measurement which could be due to uncertainties in the simulation.

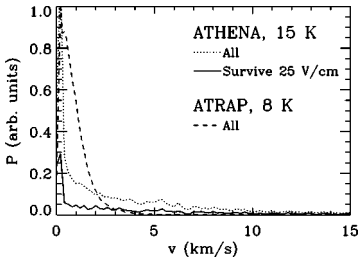

FIG. 4. The probability P for a $\bar{H}$ atom to have speed v along the magnetic field; the thermal speed perpendicular to the field is 0.5 km/s at 15 K. For the ATHENA geometry, the solid line is for atoms that can survive a 25 V/cm field and the dotted line is for all atoms. The plasma parameters are the same as in Fig. 3.

We attempted to simulate the distribution of binding energies in the second ATRAP geometry [3]. For this simulation, we used 0.9 mm and 1.5×10^7 cm^{-3} for the extent and density of the e^+ plasma. In Ref. [3], the $\bar{p}$'s are driven many times between two wells and have many extra chances to capture an e^+ compared to Ref. [2]. The experiment found a roughly flat distribution of atoms with stripping field in the range 20–60 V/cm. The simulation found that 76 out of 177 698 $\bar{H}$'s could survive a 20 V/cm field. Although the statistics are low, it appears that the distribution is not flat and that the atoms are mostly weakly bound. Roughly 1/3 of the atoms strip at fields between 20 and 25 V/cm. The physical origin of the weak binding is that it is easier to capture an e^+ into a weakly bound (i.e., large) state. This seems to be a real difference with experiment and it is not clear what the origin is.

The velocity of a $\bar{H}$ atom is important because it determines whether the $\bar{H}$ will travel toward a trap and how much kinetic energy will need to be removed to trap it. We show the calculated distribution of velocity of the $\bar{H}$ atoms along the magnetic field in Fig. 4. For comparison, the average speed across the field, $\sqrt{2k_BT/M}$, is roughly 500 m/s at 15 K. While the peak of the distribution is at small velocity, a large fraction of the atoms have greater than thermal velocity. For the $\bar{H}$ atoms that can survive 25 V/cm fields, roughly 1/2 have speeds greater than 2000 m/s in the ATHENA geometry. The directionality of the $\bar{H}$ atoms could be useful for trapping. However, it appears that it will be necessary to remove a few km/s from a typical $\bar{H}$ in order to capture them. Note that the velocity along the field is not as high for the ATRAP geometry. This is due to the smaller thickness of the e^+ plasma; a $\bar{p}$ needs to be moving slower to have a chance at capturing an e^+. Thus, a very thin plasma

has the advantage of producing slower $\bar{H}$ atoms.

III. ANTIPROTON SLOWING AND POSITRON HEATING

We will now discuss important aspects of the simulation. For both experiments, the $\bar{p}$'s start with high speeds and then slow down through the range where they can capture an e^+. It is important to model this slowing, at least qualitatively, because the speed of the $\bar{p}$ along the **B** field determines the time available for it to neutralize in the e^+ plasma and determines the binding energy of the resulting $\bar{H}$ atom. Also, the speed determines the direction the $\bar{H}$ travels after recombination and how easily it can be captured in a trap. Finally, the energy lost by the $\bar{p}$'s can raise the temperature of the e^+ plasma.

At higher energies, $\bar{p}$'s are most effectively slowed by the excitation of plasma oscillations. We used the formulation of the stopping power of a magnetized electron plasma in Ref. [17]; the energy lost during one pass through the plasma is obtained from the computed energy lost per unit length [Eq. (8) of Ref. [17]] times the plasma thickness. The wavelength of the plasma oscillations was chosen to be between $5e^2/(4\pi\varepsilon_0 k_B T)$ and the smallest length dimension of the plasma. The stopping power was not strongly dependent on the value of these limits. The lower limit for the wavelength of plasma oscillation means the energy change due to close collisions with individual e^+'s are not included in this method and, thus, needed to be simulated using the method described below. We did not include the fluctuations of the plasma waves as possible source of energy change of the $\bar{p}$'s. This is not a bad approximation when the kinetic energy of the $\bar{p}$'s is larger than the thermal energy of an e^+. However, when the $\bar{p}$'s have roughly $k_B T$ of kinetic energy, then not including the fluctuations becomes a problem. Including the fluctuation of energy change due to the plasma oscillations is beyond the scope of our simulations, but we did not want to have the velocity of the $\bar{p}$'s artificially damp to 0. Therefore, whenever the kinetic energy of $\bar{p}$'s became $\sim k_B T$, we turned off the slowing due to plasma waves since excitation of plasma waves is simply another mechanism for bringing the $\bar{p}$'s into thermal equilibrium with the e^+ plasma.

The energy lost or gained by collisions with individual e^+'s was obtained by numerical simulations. The close collisions were simulated by firing e^+'s along the magnetic field line at the moving $\bar{p}$. The e^+'s were given a thermal distribution and random impact parameters that covered the spatial region neglected in the calculation of slowing due to plasma waves. To compute the energy transfer for a scattering event, we solved the classical equations of motion numerically where the $\bar{p}$ was allowed the full three-dimensional motion; the e^+'s were allowed the full motion along the magnetic field but the motion perpendicular to the field was solved using the guiding center approximation including the $\vec{E}\times\vec{B}$ drift. This scattering more strongly affects the cyclotron motion of the $\bar{p}$'s. Because the e^+'s mainly move along the magnetic field, the momentum transfer to the $\bar{p}$ is mostly perpendicular to the magnetic field.

Finally, the $\bar{p}$ energy can change due to capture of an e^+ into weakly bound states that can not survive in the several V/cm electric fields in the traps [18]. For example, if the e^+ plasma is at potential V_0 and the $\bar{H}$ is stripped at a position where the potential has decreased to V_s, then the $\bar{p}$ loses energy equal to $e(V_0 - V_s)$. Within our simulation, this is the only mechanism in the simulation that can cause a $\bar{p}$ to drop to energies that cannot reach the e^+ plasma. This also has the effect of giving potentially large changes in the radial position of the $\bar{p}$'s in the trap because the $\bar{H}$'s can cross magnetic field lines. We simulate both the change in energy and radial position by numerically computing the strongest electric field that the $\bar{H}$ can survive (this is accomplished by ramping an electric field in the direction of the magnetic field as described above). We then follow the motion of the $\bar{H}$ through the trap. The average motion is assumed to be a straight line and we use the velocity numerically averaged over several cyclotron periods of a $\bar{p}$ to compute the trajectory.

The radial motion of a $\bar{p}$ causes uncertainties in our calculations for the ATHENA experiments because the e^+ plasma has a relatively small radial extent. The radial position changes due to capture and stripping of an e^+. Also, the radial position can change if the electric fields are not cylindrically symmetric. This is impossible to simulate since small asymmetries would cause substantial position drift during the several thousand (up to 10^5) oscillations that a $\bar{p}$ makes in the Penning trap (see the shape of the potential in Fig. 1). We assume that any asymmetries in the electric field that cause $\bar{p}$'s to drift out of interaction with the e^+ plasma would cause others to drift into interaction.

The $\bar{p}$ slowing can cause the temperature of the e^+ plasma to rise. The full simulation of the evolution of the e^+ plasma temperature is beyond the scope of this paper, but we can roughly estimate the range of temperature variation. For each increment of energy per e^+ added to the plasma, the temperature rises by roughly $\Delta E/3k_B$ if we neglect cooling mechanisms. For the ATHENA experiment, the ratio of the number of e^+'s to $\bar{p}$'s is roughly 10^4; thus, the temperature of the plasma rises by roughly 3 K for each 10 eV a $\bar{p}$ loses to the plasma. However, the plasma does cool during this process which means the temperature change of the e^+ plasma is small for the ATHENA experiment. In the first ATRAP configuration [2], the ratio of e^+'s to $\bar{p}$'s is roughly 2–10. The $\bar{p}$'s start with an energy roughly 5 eV above the plasma and cool over a time roughly $100\times$ longer than the e^+ radiate away the excess energy. This implies that the e^+ temperature rises by 20–100 K. Estimates for the second ATRAP configuration [3] are more uncertain because both the starting energy of the $\bar{p}$'s and the time needed to lose energy in the plasma are not known. (In this geometry, the $\bar{p}$'s are gently heated in each well until they can reach the e^+ plasma.) The number of $\bar{p}$'s roughly equals the number of e^+. Guessing that the energy of the $\bar{p}$'s is between 1 and 5 meV gives a temperature change of 4–20 K if the $\bar{p}$ slowing time is comparable to the e^+ radiation damping time.

IV. CONCLUSIONS

In conclusion, simulations of the three-body capture was able to roughly reproduce the reported fraction of recombi-

nations from both of the experiments on antihydrogen formation. We also find that the recombination fraction does not decrease strongly with the temperature of the e^+ plasma in agreement with measurements [12]. The only point of qualitative disagreement is with the energy distribution of $\bar{H}$ binding energies: the experiments [3] obtain a roughly flat distribution but the simulations give a distribution peaked at weaker binding. The origin of this disagreement is unknown.

The simulations suggest the importance of the arrested nature of the capture process due to the small thickness of the e^+ plasma. The short interaction time of a $\bar{p}$ with the e^+ plasma causes a large fraction of the antihydrogen to have binding energy less than the minimum, steady-state binding energy: $8k_BT$. In their current configuration, the e^+ cloud in the ATHENA experiment has a larger extent and higher density than in the ATRAP experiment. This is the main factor for giving more deeply bound atoms in the ATHENA configuration because it allows additional e^+-$\bar{H}$ collisions. A substantial population of $\bar{H}$ travels mainly along the field which means they can be directed to a trap. Unfortunately, this also means that the $\bar{H}$ have speeds from a few hundred m/s up to several km/s which will make them difficult to stop.

The main uncertainties in our simulations are the temperature of the positron plasma for the ATRAP experiments and the radial drift of the $\bar{p}$'s in the ATHENA experiments. We expect that both of these uncertainties affect our results at a quantitative level but do not change the general trends displayed in our simulations.

ACKNOWLEDGMENTS

I gratefully acknowledge extended conversations with J. D. Hanson and L. D. Noordam; I also thank the ATHENA (in particular J. S. Hangst) and the ATRAP (in particular P. K. Oxley and G. Gabrielse) Collaborations for giving detailed information about the traps and the plasmas. This work was supported by the Chemical Sciences, Geosciences, and Biosciences Division of the Office of Basic Energy Sciences, U.S. Department of Energy. Computational work was carried out at the National Energy Research Scientific Computing Center in Oakland, CA.

[1] M. Amoretti *et al.*, ATHENA Collabration, Nature (London) **419**, 456 (2002).
[2] G. Gabrielse *et al.*, ATRAP Collaboration, Phys. Rev. Lett. **89**, 213401 (2002).
[3] G. Gabrielse *et al.*, ATRAP Collaboration, Phys. Rev. Lett. **89**, 233401 (2002).
[4] G. Gabrielse, S.L. Rolston, L. Haarsma, and W. Kells, Phys. Lett. A **129**, 38 (1988).
[5] M.E. Glinsky and T.M. O'Neil, Phys. Fluids B **3**, 1279 (1991).
[6] F. Robicheaux and J.D. Hanson, Phys. Rev. A **69**, 010701 (2004).
[7] At any point in the trap, two $\bar{p}$'s can collide and transfer energy between cyclotron motion and motion along the **B** field, but this is not an important process for the reported experiments.
[8] The $\bar{p}$'s heat the e^+ plasma during the experiments. For the ATHENA geometry, the larger number of e^+'s means the temperature does not rise much. For the ATRAP geometry, we estimate that the e^+ plasma rises by roughly 20–100 K in Ref. [2] and roughly 5–20 K in Ref. [3].
[9] P. Mansbach and J. Keck, Phys. Rev. **181**, 275 (1969).
[10] Reference [5] investigated the time dependence of the binding energy distribution. The present results appear to agree with Ref. [5] for longer times but do not agree at shorter times because they start with a distribution of bound e^+ with binding energy up to k_BT while the current simulations start with no bound e^+'s.
[11] M. Amoretti *et al.*, ATHENA Collaboration, Phys. Lett. B **578**, 23 (2004).
[12] M. Amoretti *et al.*, ATHENA Collaboration, Phys. Lett. B **583**, 59 (2004).
[13] F. Robicheaux and J.D. Hanson, Phys. Plasmas **10**, 2217 (2003).
[14] T.C. Killian, M.J. Lim, S. Kulin, R. Dumke, S.D. Bergeson, and S.L. Rolston, Phys. Rev. Lett. **86**, 3759 (2001).
[15] There are a few $\bar{p}$ that reach low velocities ~1–10 m/s and experience long interaction times. However, these atoms typically have velocities perpendicular to the **B** field that are 10–100 times larger than the velocity parallel to the field; thus, the slow atoms annihilate on the walls of the trap near the e^+ plasma and do not reach the region where the $\bar{H}$ atoms are detected.
[16] G. Gabrielse (private communication).
[17] H.B. Nersisyan, M. Walter, and G. Zwicknagel, Phys. Rev. E **61**, 7022 (2000).
[18] We compute the electric fields and potentials in the traps using the experimental values of the voltages on the electrodes and the estimated peak density of the positron plasma. The fields and potentials are computed self-consistently with the plasma density profile using the thermal distribution in a magnetic field.